Leadership in Sustainable Infrastructure

Leadership en Infrastructures Durables

Vancouver, Canada

May 31 – June 3, 2017/ *Mai 31 – Juin 3, 2017*

NUMERICAL MODELING OF THE FLOW HYDRODYNAMICS AND FLOATING DEBRIS PATHWAYS AROUND THE BEQUIA ISLAND

Philippe April LeQuéré [1,4], Ioan Nistor [2], and Ronald Townsend [3]
[1, 2, 3] University of Ottawa, Canada
[4] papri010@uottawa.ca

ABSTRACT

To accommodate an increasing number of tourists visiting Bequia, the largest island of Saint-Vincent and the Grenadines, the local government constructed an airport, through a major coastline land-reclamation project. However, due to the prevailing ocean current patterns in the area, an inlet created on the East side of the new airport is prone to trapping significant amounts of ocean-borne debris. This litter accumulation creates a health risk to local fishermen who clean their daily catch using water from the inlet. It is proposed to install a rock-fill groyne structure on the eastward side of the new inlet to address this problem. The utilisation of a coast-line groyne in this case is somewhat unorthodox, as the latter is normally employed to mitigate against coastal erosion.

The goal of this study is to optimise the groyne design with the assistance of a 3D numerical model. The 'Delft3D' open-source model (WAVE and FLOW modules) was selected to examine the effects of different orientations and lengths of the proposed groyne on the movements of floating debris. Included in the initial phase of the study was a field investigation to collect certain data which was necessary for model calibration and validation. This involves the use of an Acoustic Doppler Current Profiler (ADCP) to measure local shore bathymetry and also current velocities over a range of tidal cycles. This paper reports on the preliminary results of this study.

Keywords: - Bequia, numerical model, Delft3D, hydrodynamic, tide-induced current, groyne

1. INTRODUCTION

This paper focuses on the numerical modeling exercise undertaken of the coastal region of the Paget Farm community on the island of Bequia, Saint-Vincent and the Grenadines. This particular region is being studied in order to address the problem of floating debris accumulation that is occurring in the Jeff Gregg inlet. This new coastal inlet was created in the process of constructing the new J.F. Mitchell airport on the island in 1990. Because the airport is sited on new land reclaimed from the ocean, the resulting modified coastline in this area has changed the local coastal hydrodynamics and ocean bed morphology. These changes have been found to be largely responsible for the aforementioned accumulation of floating ocean-borne debris in the Jeff Gregg inlet, which is located immediately east of the airport. The prevalent winds and wave directions are mostly from east to west in the area and hence the resulting ocean surface currents tend to capture and transport marine debris (sargassum, Paget Farm community litter, etc) into the Jeff Gregg inlet

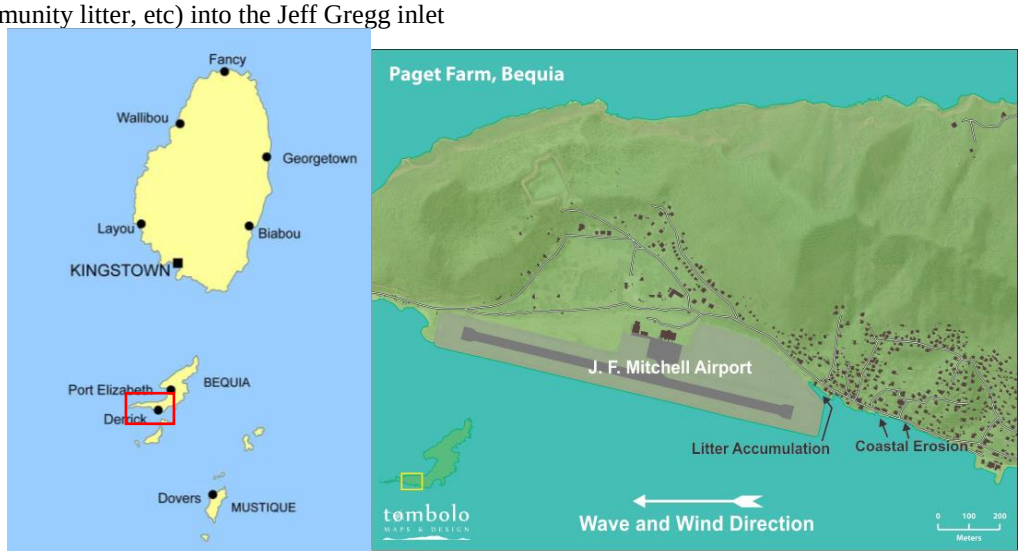

Figure 1 Paget Farm Coast Map (Tour du monde en images. 2015)

The goal of the study is to redirect the prevalent surface current in this area (and with it the related path of debris) away from inlet entrance and towards the main (bypass) ocean current. This will be accomplished by building a rubble mound groyne just east of the inlet. Optimizing the design of this structure will require a better understanding of the existing coastal hydrodynamics and the related debris movements in the area. This will be accomplished with the aid of a dedicated 3-D mathematical model of the ocean region in question. The model selected for this exercise is the Delft3D numerical model, which is a software that is particularly well-suited for studying complex coastal hydrodynamics. Very little information is available about this remote region. Accordingly, a field campaign was initiated to gather the necessary information to build and calibrate the model.

2. THE DELFT3D MODEL

As previously stated, a computational model of the coastal area in question was developed using the open source of Delft 3D. This software is capable of simulating the coastal hydrodynamics using a module called FLOW, by solving an approximation of the Navier-Stokes equations for incompressible shallow water flow (Deltares, Delft3D-FLOW. 2011) (Trouw et al. 2012) (Visser, 2002). FLOW can interpret the effects of wind, tide and other defined inputs and outputs on water. However, it cannot simulate the effect of waves. The waves are therefore modeled as forcing factors on the surface grid layer into the FLOW simulation. These factors are calculated by the WAVE module, which will be presented later. Figure 2 illustrates the computational grid used in the FLOW module, superposed onto Bequia's map:

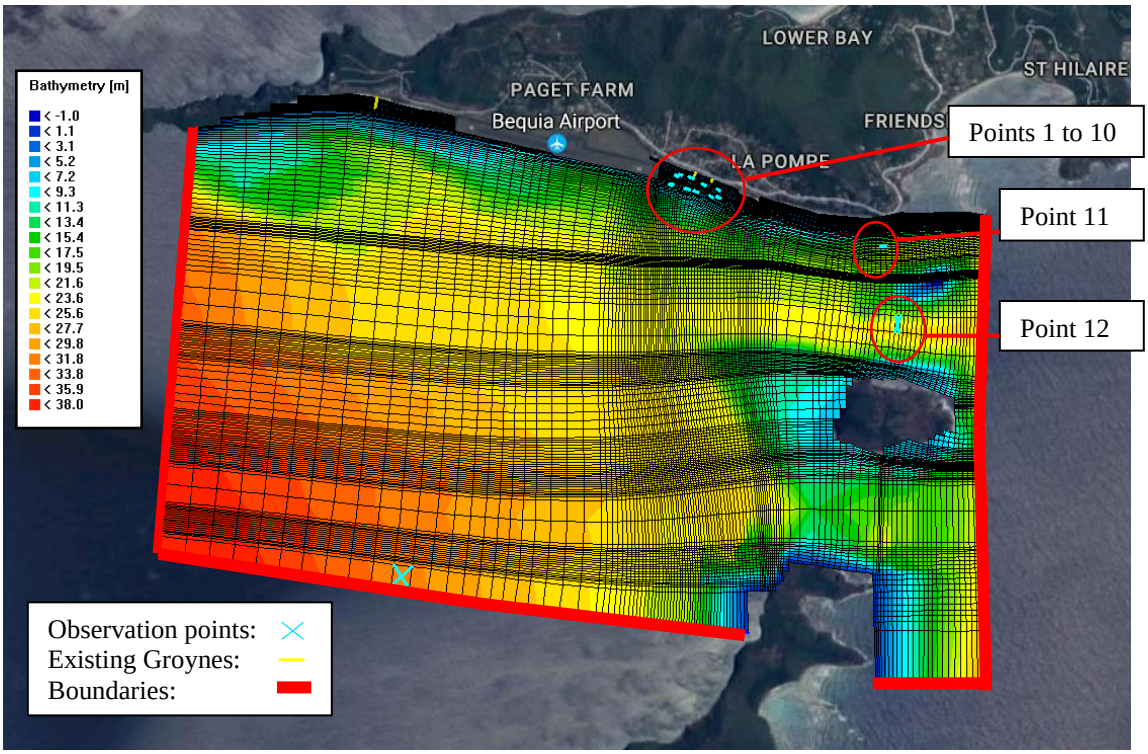

Figure 2: FLOW Module Grid

Shown in yellow in the legend, are existing groynes that were found along this particular section of the coastline. The offshore boundaries (shown in red) were defined as a sinusoidal function that mimics the effect of the tide at the boundaries. A total of 14 Eulerian points, called observations points, were also defined at the approximate locations where velocity measurements were taken in the field (see the Data Collection section). Points 1 to 10 were used for roughness calibration while points 11 and 12 were used for tide-induced current calibration. Two additional points at the south and east boundaries were used for the monitoring of the tide at corresponding locations to ensure that the correct variation of the tide cycle was simulated. The grid is a 3D grid with 121 cells in the X-direction, 153 in the Y-direction and 6 in the Z-direction, for a total of 111,078 cells. The horizontal grid was refined around the islands within the grid domain because of the effect it had on the tide-induced current. The vertical cells get smaller when closer to they are water surface or to the sand bottom. They are expressed as percentages of the water depth, causing the cells to also be smaller when closer to the shore.

The wave simulation is done with the WAVE module and the calculated forces are then communicated to FLOW for the hydrodynamic simulation. These wave forces are calculated using a specific wave model called SWAN (Simulating Waves Nearshore) (Deltares, Delft3D-WAVE. 2011) (Visser. 2002). This model uses the linear wave theory to derive the necessary equations.

3. FIELD MEASUREMENTS

In order to run Delft3D-FLOW with Delft3D-WAVE modules, the following information is necessary: depth of the whole area of interest, characteristics of the tide, bottom roughness, wind and waves. A good understanding of the mechanisms that generate currents is also very useful. Details on current velocities at multiple locations under known conditions are also necessary to calibrate the numerical model.

Forecasts for wind, wave and tide for the Friendship Bay, which is located two kilometers east of the airport, were obtained on the website www.wisuki.com The daily field data observations undertaken by the authors over two separate field campaigns of data collection were used for the calibration of the model and some of the historical values will be also used for the design of the groyne. The historical values indicate that the wind's nautical direction is always between 70 and 100 degrees of North and have a typical velocity of 10 m/s. The waves are also always coming from the same direction with a typical swell significant height between 1 and 2 meters. The tide in the area is semi-diurnal with maximum amplitude of 0.7m. As well, a navigation map of the area was employed, which provides approximate bathymetry of the region. This map was useful for the coarser regions of the model grid.

However, it was not precise enough for those areas closer to the shore. To address this deficiency, two field campaigns were conducted to collect the necessary data. The first necessary data were detailed bathymetry measurements which were carried out along the near-shore region. An acoustic Doppler current profiler (ADCP) was used to collect this information. This device can be used to generate a bathymetric map using its transducers to get the depth (Z coordinate) and an integrated GPS unit to get X and Y coordinates as well as correcting the depth with elevation variations caused by waves and changes of tide. Over the course of the campaign, a total of 23400 x-y-z points were collected and were used to construct the model's grid. Continuous bathymetry measurements in the study area were obtained using the ADCP unit tethered to a boat. Figure 3 shows the area that was surveyed in these exercises.

Figure 3: Field Measurements – Schematic of the Depth Transects

Eulerian point velocities in the water column were also collected to assist in the calibration of the model. Using the ADCP, velocity can be measured using the transducers that compare the reflection of sound waves on small particles in the water column between two time steps. This provides point velocities through the entire water column. The boat was anchored at a particular location which was then identified using GPS. GPS was also used to correct velocities by adjustments that reflected movements of the boat. In order to use these points in the calibration of the model, the velocities were averaged over time to account for fluctuations due to the waves and the movement of the boat. Since the software used (ADCP post processing program) could not separate the velocity in the Z direction at any given time step, the velocity was also averaged over the whole water column. A total of 29 points were collected. Table 1 summarizes some of the points that were collected on August 29th 2016.

Time	Depth (m)	Velocity X (m/s)	Velocity Y (m/s)	Time of Measurement (s)	UTM(m)	UTM(m)
7:03:02	2.16	-0.055	-0.002	80	689243.04	1436328.50
7:05:11	2.66	-0.038	0.017	64	689238.87	1436322.48
7:10:53	2.08	-0.068	-0.036	77	689319.94	1436308.85
7:15:16	3.28	-0.118	-0.038	79	689397.92	1436262.99
7:19:13	3.29	-0.120	-0.034	74	689477.33	1436238.94
7:23:15	5.00	-0.170	-0.057	103	689485.18	1436189.92
7:27:31	5.67	-0.162	-0.059	85	689438.65	1436193.31
7:31:56	5.53	-0.144	-0.051	88	689351.88	1436223.49
7:35:46	5.70	-0.154	-0.038	75	689286.46	1436243.29
7:39:44	5.96	-0.127	0.004	83	689182.92	1436269.85

Table 1: Example of Velocity Points

Each point has a location defined in the UTM (Universal Transverse Mercator coordinate system) which helped trace back its exact position on the numerical model grid. The velocities at those points were converted into X and Y components for an easier comparison with the model's results.
However, two important ingredients for the model construction were still missing, namely, the bottom roughness and the tide-induced current. As the bottom roughness can vary on a case- by- case basis, calibration is necessary. Also, during the first site visit, it was observed that there was a strong current between the islands located east of the airport and that its direction changes with the reversal of tide. At flood tide, the current moves from east to west, but with an ebb tide, the current moves from west to east. Knowing that the current direction changes depending on the instant of the tide, the latter is the most likely driving factor for the current phenomenon. The way that this was simulated in the model was by defining the east boundary as a harmonic water level and the west boundary as a harmonic total discharge. This is described in more detail in the calibration of the tide-induced current section. However, no data is available for the velocity of this current under any given tide condition. Therefore, a calibration using the measured depth-averaged velocities at the given points is needed in order to calibrate the boundary condition. Figure 4 illustrates the direction and the location of the tide-induced current:

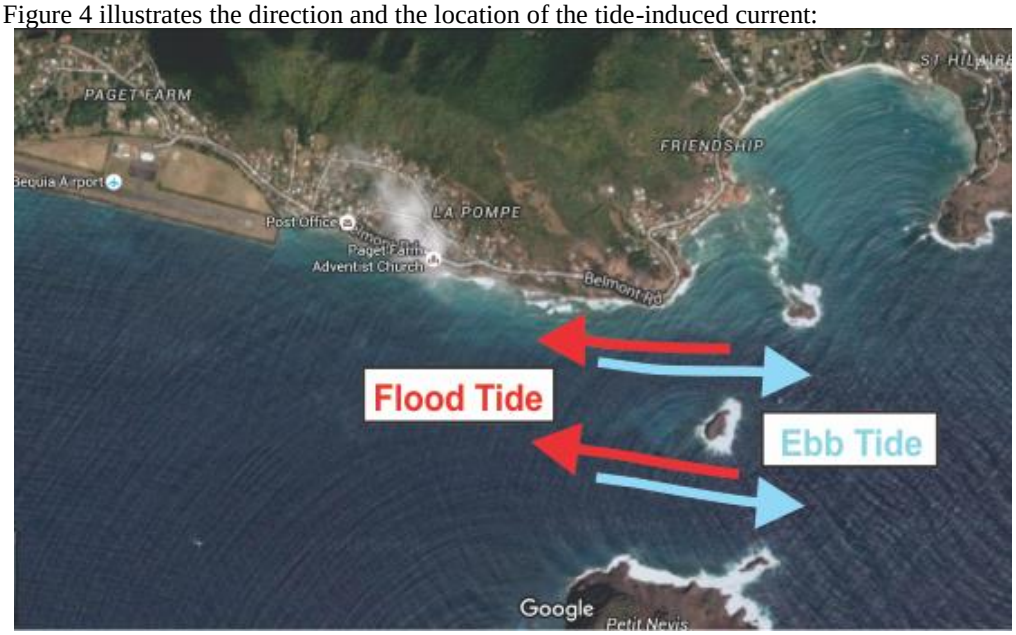

Figure 4: Tide-Induced Current

The movements of floating debris were observed during the velocity measurements just east of the inlet. It was noted that the debris were moving approximatively parallel to the shore and were moving westward even when the current was moving eastward. This indicates that the tide-induced current isn't the main driving factor of the surface current. Due to time constraints, the measurements were limited. If more time had been available, a tracking of floating debris, using GPS placed on floaters released at different times and sea conditions, could have extended the information available to validate the model. Also, a time series of the depth-averaged velocity over a full tide cycle at a location where the tide-induced current creates high velocities (such as point 11 or 12 in Figure 2) would have been preferable to create a better numerical estimation of the phenomenon.

4. CALIBRATION OF THE MODEL

Because data on the bottom roughness and the tide-induced currents are missing, the model needs to be calibrated. It was decided to separate the calibration by adjusting two model parameters: one for the tide-induced current and one for the bottom roughness.

Calibration of the Tide-Induced Current

The tide-induced current is modeled by defining the east boundary as a harmonic water level and the west boundary as a harmonic total discharge. Delft3D has a function called harmonic boundary where a defined value for water level (or total discharge in this case) varies following a sinusoidal function. The boundaries were defined as such because of some instability problems experienced when the two boundaries were defined as water level. The east

boundary will be modeled following the tide's amplitude and speed (degree/h) at the moment that the point velocities were measured (see Table 2). The west boundary has three components that need to be controlled: the total discharge for the west boundary and that for the south boundary and the lag between the east boundary and the west boundary harmonic cycles. The total discharge was defined by the authors as a factor of the tide amplitude so it that varies proportionally when the tide amplitude is changed.

As the calibration process, by adjusting the bottom roughness, is intrinsically related to the calibration of the tide-induced current and vice versa, a value for the bottom roughness has to be assumed to first obtain a preliminary value for the boundaries' parameters. For simplicity, the bottom roughness value for the calibration of the tide-induced current was assumed to be the same in the whole region. From scuba dives performed by the authors in the area, it was observed that, except near the shore, the ocean bottom in the area is covered mostly by sand. Samples of the sand were collected and analysed. The resulting grain-size distribution curves provided representative D_{50} – values for the three samples collected. The Manning's roughness value for the ocean bed was then calculated to be n = 0.018, using the following formula: (California Departement of Water Resources. 1970)

[1] $n \approx 0.039 * D_{50}^{\frac{1}{6}}$

The required data on wave conditions, tide amplitude and wind conditions were obtained on the web site www.wisuki.com, where daily information on the local weather is continuously updated. As point velocities were recorded over two different days, under different weather conditions, two calculations were required. The following table summarizes the tide, wave and wind conditions for those two days:

	Date	August 21st	August 22nd
Wave condition	Significant height (m)	0.8	0.8
	Direction (d)	90	120
	Period (s)	8	8
Wind Condition	Speed (m/s)	5	5
	Direction (d)	90	90
Tide condition	Time/Water Level	2:30 +0m	3:07 +0m
		8:38 +0.4m	9:24 +0.4m
		15:16 +0.1m	16:30 +0m
		20:23 +0.3m	21:27 +0.3m

Table 2: Information required for the model's Tide Lag Calibration (wisuki. 2016)

The tide-induced current was calibrated using the velocity measured on those two days at approximatively the same location which is between Bequia and Middle Cay and between Middle Cay and Petit Nevis (Points 11 and 12 in Figure 2). Figure 5 summarizes the results of the calibration:

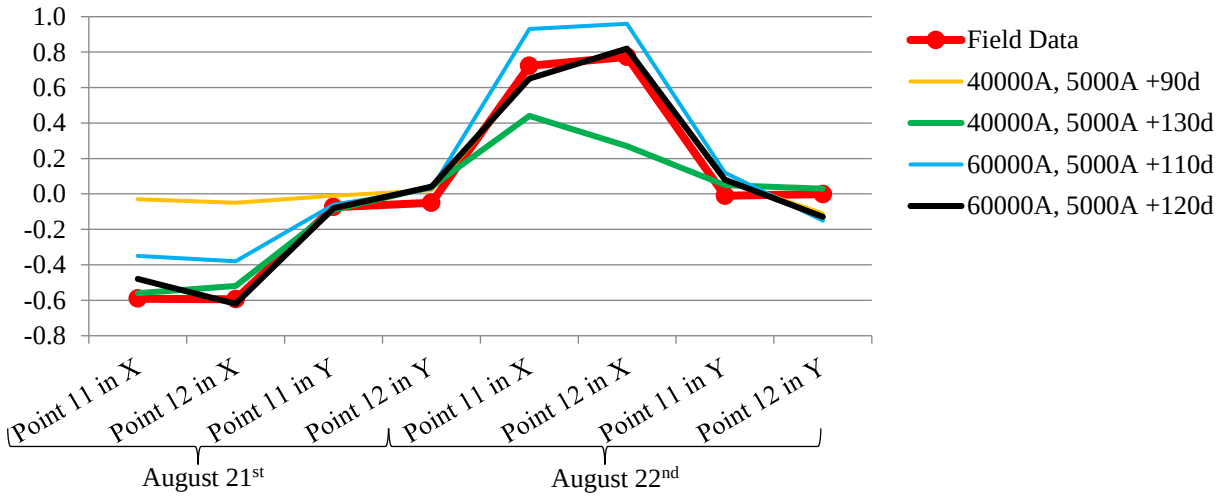

Figure 5: Tide Calibration Results

After analysing the data, it was observed that a total discharge for the west and south boundaries, of 60000 times the tide amplitude and 5000 times the tide amplitude respectively, represents most accurately the tide-induced current. A lag between the definitions of the two boundaries of 120 degrees was also found to be more appropriate. A root mean square error of 0.083 m/s was calculated. The main source of that error stems from the fact that the measured velocities at points 11 and 12 under the two conditions are similar and almost identical when considering velocities in the Y-direction. In the numerical model, point 11 exhibits lower velocities in the X-direction while the velocities in the Y-direction indicate that the currents are not parallel. This can probably be attributed to the uniform conditions for the eastern boundary.

Calibration of the Bottom Roughness

As soon as the tide lag was correctly reproduced, the second element used in the calibration is the bottom roughness. When diving in the area for visual confirmation of the nature of the bottom terrain, it was observed that the bottom near the coast (within 100m of the shore) consisted of small reefs and sand patches. This fact was also observed via satellite imagery. As there is no precise information on a Manning's roughness for that type of bottom, the bottom roughness adopted for this region will have to rely on a calibration process. As a reference, Manning's roughness was estimated as high as 0.22 for some reef systems in earlier similar-type studies (Cialone et al. 2007). For the rest of the grid, the roughness was assumed to be constant with a Manning's n = 0.018, a value that was used to verify tide lag calibration. At a specific distance, the bottom roughness was assumed uniform with a Manning's n = 0.018 and the roughness was then increased close to shore as needed. As all the measurements used for this calibration were taken on the same day, only one sea condition was used in the model. Table 3 summarizes the wave, tide and wind information inputted into the model:

	Date	**August 29th**
Wave condition	Significant wave height (m)	1.2
	Direction (d)	90
	Wave period (s)	7
Wind Condition	Speed (m/s)	7
	Direction (d)	90
Tide condition	Time/Water level	3:14 +0.2m
		8:23 0m
		15:03 0.5m
		23:03 0m

Table 3: Model Information for Roughness Calibration (wisuki. 2016)

As the data was collected between 7:00AM and 7:40AM on August 29th 2016, only the ebb tide between 3:14AM and 8:23AM will be simulated. The points used for the calibration are shown in Figure 2 and marked from 1 to 10. All these points are very close to the location of the intended groyne. The following table summarizes the results of the calibration for bottom roughness:

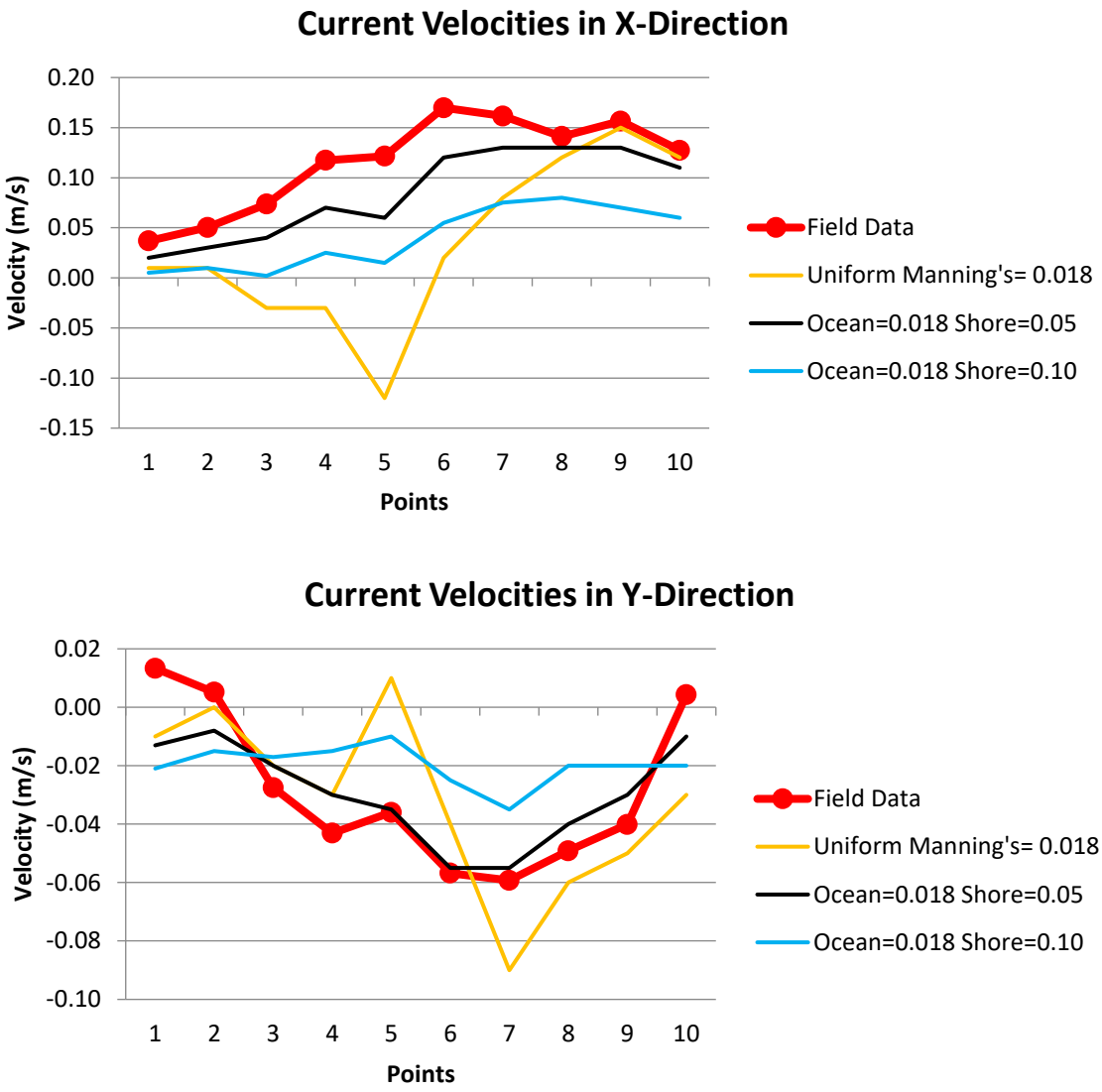

Figure 6: Bottom roughness Calibration

After analysing the data, it was observed that when the bottom roughness for the first 100m of shore is increased to a Manning's coefficient of 0.05, while keeping the rest of the grid at 0.018, the model was most accurately representing the field measurements. The calculated root mean square error is 0.0264 m/s. This difference is acceptable since it is within the mean averaging error of 0.048 m/s for the data set. Also, the model is representing correctly the trend of the measured velocities. This gives a good indication that it will accurately model the movement of the floating debris. Knowing that the shore is composed of a mix of small reefs and sand, it is in line with previous studies that have also found that a reef bottom will have a higher roughness. (Cialone et al. 2007) Previous authors have also suggested similar Manning's coefficient for reefs systems in shallow water. (Rosman et al. 2011) (Prager. 1991)

5. VALIDATION OF THE MODEL

Validation of the model was done by tracking the movement of floating debris and testing if the surface current along the shore will push the debris toward the inlet. This is done by releasing floating buoys, defined as drogues by Delft3D. It was observed that using the default value of JONSWAP's bottom friction in Delft3D (0.067 m^2s^{-3}), the

debris are moving offshore perpendicularly to the shore. This observation is contrary to what was observed during the field campaigns. So, different values of JONSWAP were tried and it seems that a lower value is more appropriate for this situation of 'shallow water with reefs' bottom. This confirms the newest findings that the assumed value of JONSWAP for wind driven waves is too high. (Cialone et al. 2007) Figure 7 illustrates the movement of floating debris released at 3 locations every hour during a full tide cycle.

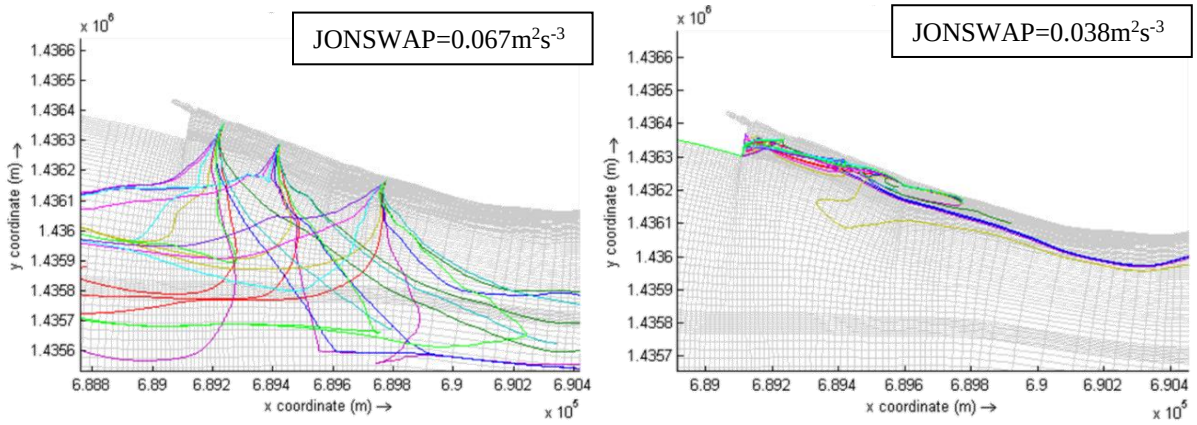

Figure 7: Floating Debris with Different JONSWAP

A JONSWAP parameter of 0.038 m^2s^{-3} will be used as it was proposed as a more appropriate value for this situation and represents better what was observed. (Vledder. 2010) However, the value of JONSWAP can't be adjusted further since no actual floating debris tracks were measured in the field. The change of JONSWAP has had little effect on the depth-averaged velocity calibration and the values presented for the calibration are for the reduced JONSWAP parameter.

6. CONCLUSIONS AND WORK IN PROGRESS

A 3D hydrodynamic model Delft3D was established for the coastal region of Paget Farm on Bequia Island in St. Vincent and Grenadines, to study the wave- and tide-induced hydrodynamics of the area relevant to the movement of floating litter along the coastline. The tide-induced current was accurately reproduced. The validation of the model has confirmed findings that JONSWAP's parameter for wind driven waves is too high. Now that the calibration process is completed, the model will be used to find the optimal size and orientation of a proposed new groyne which will have a triple role: (1) protect the local coastal area against erosion, (2) provide additional landing ground for fishing boats and (3) redirect the current (and litter) away from the entrance to the inlet.

The groyne will be represented in the model as a series of 'thin dams'. (Deltares, Delft3D-FLOW. 2011) (Visser. 2002) These are cells that are defined as 'always dry'; therefore they will be excluded from the computation. Since there is no exchange of water through those cells, the velocity around these cells will be zero. This will modify the distribution of velocities around the area of the inlet and thus redirect the influx of litter away from the airport. Several scenarios will be studied in combination with assessing the influence of the groyne configuration. The final selected configuration will be further modeled to investigate the morphologic impact of the groyne. This will evaluate the assumption that a groyne has the potential to reduce the present coastal erosion eastward of the airport.

7. REFERENCES

Booij, N., Ris, R. C. and Holthuijsen L. H. 1999. A third-generation wave model for coastal regions. *Journal of Geophysical Research, Vol. 104*, p. 7649-7666.

California Departement of Water Resources. 1970. *Determination of the Manning Coefficient From Measured Bed Roughness in Natural Channels*, Washington: United States Government Printing Office.

Chatzirodou, A. and Karunarathna, H. 2014. Impacts of Tidal Energy Extraction of Sea Bed Morphology. *34th Coastal Engineering Proceedings*, Seoul, Korea.

Cialone, M. A., McKee Smith J. 2007. *Wave Transformation Modeling with Bottom Friction Applied to Southeast Oahu Reefs*, US Army Engineer Research and Development Center, Vicksburg, Mississippi.

Deltares. 2011. *Delft3D-FLOW User Manual*, Deltares, Delft, Netherlands.

Deltares. 2011. Delft3D-WAVE *User Manual*, Deltares, Delft, Netherlands.

Elias, E. 1999. The Egmond Model, Calibration, Validation and Evaluation of Delft3D-MOR with Field Measurements. Delft Hydraulics. Delft, Netherlands

Mitchell, S. J. 2016. *Bequia Airport - an essential lifeline with an even brighter future*. Consulted on March 25th 2016, http://www.iwnsvg.com/2016/01/28/bequia-airport-an-essential-lifeline-with-an-even-brighter-future/

Prager, E. J. 1991. Numerical simulation of circulation in a Caribbean-type backreef lagoon. *Coral Reefs,*10 (4): 177-182.

Rosman, J. H. 2011. A framework for understanding drag parameterizations for coral reefs. *Journal of Geophysical Research*, 33 (8): 1-15.

Tour du monde en images. 2015. *Saint-Vincent-et-*Grenadines, Consulted on January 17th 2017, http://www.jump-voyage.com/carte-saint-vincent-et-grenadines/vacances-saint-vincent-et-grenadines-1/

Trouw, K., Zimmermann, N., Mathys, M., Delgado, R. and Roelvink, R. 2012. Numerical Modelling of Hydrodynamics and Sediment Transport in the Surf Zone: a Sensitivity Study with Different Types od Numerical Models. *Proceedings of the International Conference on Coastal Engineering*, Santander, Spain

U.S. Geological Survey. 2009. *Measuring Discharge with Acoustic Doppler Current Profilers from a Moving Boat*. Reston, Virginia: U.S. Departement of the Interior.

Visser, R. 2002. Morphological modelling in the vicinity of groynes, an extended application of Delft3D-RAM including impact, Delft University of Technology, Delft, Netherlands.

Vledder, v. G. 2010. Revisiting the JONSWAP Bottom Friction Formulation. *Coastal Engineering Proceedings*, Shanghai, China, 32 : 41 in waves.

wisuki. 2016. *Statistics, Friendship Bay*. Consulted on August 22nd to August 29th, 2016, http://wisuki.com/statistics/925/friendship-bay?a_wi=4&wi_m=0&a_wa=4&wa_m=0&temp=monthly&rain=quantity